

# The Detection of Super-elliptical Inclusions in Infrared Computerised Axial Tomography

N.S.Mera<sup>1</sup> L. Elliott<sup>2</sup> and D.B.Ingham<sup>2</sup>

**Abstract:** The purpose of this study is to investigate the efficiency, accuracy and rate of convergence of an evolutionary algorithm for detecting inclusions parametrised by superellipses in non-destructive evaluation and testing. The inverse problem investigated consists of identifying the geometry of discontinuities in a conductive material from Cauchy data measurements taken on the boundary. Temperature and heat flux are measured on the outside boundary of the domain and the position and the size of a super-elliptical inclusion are determined by minimising an objective functional using an evolution strategy. The super-elliptical form allows the parametric model to characterise a variety of shapes whilst at the same time regularizing the problem by the function specification method. The boundary element method is employed in order to solve the direct problem, i.e. to calculate the boundary data for a given geometric configuration. Numerical results are presented for several test examples for both exact and noisy boundary data. The algorithm developed by combining evolution strategies, the boundary element method and super-elliptical parametrisation is found to be a robust, fast and efficient method for detecting the size and location of subsurface inclusions.

**keyword:** inclusion detection, superellipses, evolution strategy

## 1 Introduction

We consider the inverse conductivity problem which requires the determination of an isotropic object  $D$ , inclusion or cavity, contained in a domain  $\Omega$  from measured temperature,  $\phi$ , and heat flux,  $\frac{\partial\phi}{\partial n}$ , on the boundary  $\partial\Omega$ . To find defects in materials by a nondestructive testing is very important in various areas of engineering. There are many practical methods for such testing, for instance ul-

trasound scattering, X-ray computerised axial tomography (X-ray CAT), infrared computerised axial tomography (IR-CAT), electrical impedance tomography (EIT), etc. In this paper we consider the problem of detecting inclusions in a material by infrared computerised axial tomography.

In the classic problem of heat conduction, the system configuration has to be specified and the governing equation can be formulated based on the physics of the problem. Then, if the boundary conditions are given, the problem can be solved to determine the temperature distribution at each point interior to the system. A different type of problems, termed *inverse geometric problems* is obtained if part of the geometry of the system is unknown and has to be determined using additional boundary measurements. In inverse geometric problems, one wants to obtain information on defects, for example position and shape, from measurements of the temperature and heat flux on the material surface. This type of problem has numerous practical applications in nondestructive testing using infrared scanning, when one can scan the surface temperature of a body that dissipates heat to the surroundings. The inner boundary is subjected to various boundary conditions, and the purpose of performing infra-red scanning is to determine the inclusion, if one exists, at the inner boundary using the additional heat flux or temperature measurements available. This geometric inverse problem forms the theoretical basis for developing IR-CAT in competition with X-ray CAT that is now prevalent in medical technology.

It is worth noting that, although the problem of cavities detection, as stated, appears to be well-known in the field of nondestructive testing, an exact solution of the problem has not been found in the literature and numerical methods appear to be more promising. Many papers have discussed this problem from a mathematical or practical point of view and various numerical methods have been proposed, see for example Hsieh and Su (1981), Lesnic (2001), Ikehata and Ohe (2002) and Rus and Gallego

<sup>1</sup> Centre for Computational Fluid Dynamics, University of Leeds, UK.

<sup>2</sup> Department of Applied Mathematics, University of Leeds, UK.

(2002).

We note that, once the problem has been formulated as an optimisation problem, various optimisation algorithms may be used in order to locate the optimum of the object function. The efficiency of a particular optimisation method clearly depends on the form of the object function. In the problem considered in this paper the object function has a complex nonlinear and nonmonotonic structure. Moreover an analytical expression for the object function cannot be computed and numerical methods are employed in order to evaluate the object function for every possible solution of the problem. Therefore evolutionary algorithms appear to be suitable tools for optimising the object function of the problem considered since they do not require knowledge of the gradient of the object functions optimised.

Evolutionary algorithms have been used before by Mera, Elliott, and Ingham (2003) for the problem of inclusions detections but only circular inclusions have been considered. It is the purpose of this paper to consider a more general parameterisation, namely super-elliptical shapes. The real coded genetic algorithms used in Mera, Elliott, and Ingham (2003) is also replaced by a Covariance Matrix Adaptation Evolution Strategy (CMAES) since this evolution strategy is known to have a high rate of convergence for numerical optimization problems.

## 2 Mathematical formulation

We consider  $\Omega$  to be a bounded domain of  $\mathbb{R}^2$ , with Lipschitz boundary and  $D$  a subdomain compactly contained in  $\Omega$ . The constant conductivity tensor  $K$  of the domain  $D$  is non-dimensionalised with respect to the conductivity tensor of the domain  $\Omega - D$ . Thus we assume that the conductivity tensor  $K$  is symmetric and positive definite, whilst the medium  $\Omega - D$  is isotropic with conductivity  $I$ . We note that if  $K = kI$  then the medium  $D$  is isotropic. Further, if  $k = 0$  the problem considered reduces to the detection of a cavity.

The refraction (transmission, conjugate) problem for the temperature  $\phi$  is given by

$$\nabla \cdot ((I + (K - I)\chi_D)\nabla\phi) = 0, \quad \text{in } \Omega \quad (1)$$

$$\phi = f, \quad \text{on } \partial\Omega \quad (2)$$

subject to refraction conditions related to the continuity of the temperature  $\phi$  and its heat flux densities  $(\partial\phi/\partial\mathbf{n}^-)$  and  $(K\nabla\phi) \cdot \mathbf{n}^+$  across the interface  $\partial D$ , where  $\mathbf{n}, \mathbf{n}^-$  and

$\mathbf{n}^+$  are the outward unit normals to the boundaries  $\partial\Omega$ ,  $\partial(\Omega - D) - \partial\Omega$  and  $\partial D$ , respectively and  $\chi_D$  is the characteristic constant of the domain  $D$ .

Assuming that  $K$  is known, the inverse conductivity problem requires the determination of  $D$  from the knowledge of the Dirichlet-to-Neumann map. In the following section we estimate the size and position of the unknown inclusion  $D$  from one boundary measurement i.e. we assume that the domain  $D$  is unknown and has to be determined if the following additional boundary condition is specified

$$\frac{\partial\phi}{\partial\mathbf{n}} = h \quad \text{on } \partial\Omega \quad (3)$$

The inclusion detection problem can be reformulated as an optimisation problem if for a given possible solution  $D$  for the cavity the direct problem (1)-(2) is solved to evaluate the heat flux on the outer boundary  $\phi'_{calc} = \left. \frac{\partial\phi}{\partial\mathbf{n}} \right|_{\Gamma}$ . Then the solution to the problem may be found by minimising the functional

$$J(D) = \|\phi'_{calc} - q\|_{L^2(\Gamma)} \quad (4)$$

where  $q$  is the measured heat flux on the outer boundary. The domain  $D$  can be parameterised in different forms, and the parameters characterising the shape, location and size of the cavity are determined by minimising the functional (4). In this paper we only investigate the cases of superelliptical inclusions, but similar solution methods may be developed for any shape for which the uniqueness of the solution is guaranteed.

## 3 The super-elliptical parameterization

Previous studies investigating the use of evolutionary algorithms for inclusions detection have only considered circular inclusions, see Mera, Elliott, and Ingham (2003). Elliptical parametrizations have also been considered for the case of cavities detection in Mera, Elliott, and Ingham (2002). It is the purpose of this study to consider more a general parameterisation, namely the super-elliptical parameterisation given by

$$\left| \frac{x - x_0}{a} \right|^p + \left| \frac{y - y_0}{b} \right|^q = 1 \quad (5)$$

or parametrically by

$$x = x_0 + a \cos^{2/p}(t)$$

$$y = y_0 + b \cos^{2/q}(t) \quad (6)$$

in the first quadrant and by symmetry in the other quadrants. Thus, the problem of identifying the inclusion  $D$  is reduced to identifying the parameters  $x_0, y_0, a, b, p$  and  $q$ . It should be noted that if  $p = q = 2$  we obtain an ellipse while if  $p = q = 2$  and  $a = b$  we obtain the circular case. When  $p$  and  $q$  are increased the superellipse is approaching a rectangular shape.

Figure 1 presents several shapes that can be represented using the formula (5) for various values of the parameters. Thus, using super-elliptical representations we are able to characterise a large variety of shapes using a small number of parameters. In order to increase the flexibility of the parametrisation we also allow the inclusion to be rotated at an angle  $\theta_0$  which becomes the 7<sup>th</sup> parameter to be identified by the optimisation algorithm. Gielis (2003) has considered a further generalization of the superellipse that gives rise to curves with  $m$ -fold rotational symmetry which can be used for identifying for example triangular, pentagonal or starlike shapes. However, this is not considered in this study which is restricted to objects with two-fold rotational symmetry.

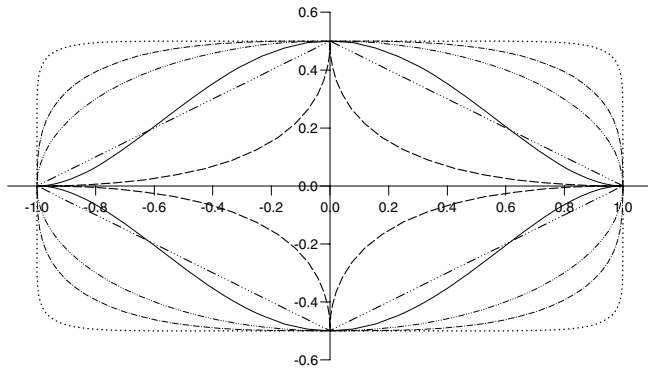


**Figure 1** : Superellipses obtained for various values of the parameters  $p$  and  $q$ , namely  $p = q = 10$  ( $\cdots\cdots$ ),  $p = q = 3$  ( $-\cdots-\cdots$ ),  $p = q = 2$  ( $-\cdots-$ ),  $p = q = 1$  ( $-\cdots-$ ),  $p = q = 0.5$  ( $---$ ) and  $p = 2.0, q = 0.5$  ( $---$ )

#### 4 The Covariance Matrix Adaptation Evolution Strategy (CMAES)

Once the problem has been reformulated as an optimisation problem, various optimisation algorithms can be employed in order to minimise the objective functional (4).

The Evolution Strategy with Covariance Matrix Adaptation (CMAES), see Hansen and Ostermeier (2001) is efficient for problems for which derivative based methods may fail due to a rugged search landscape presenting multiple discontinuities, sharp bends, noise and local optima. Similar to quasi-Newton methods the CMAES estimates the inverse Hessian matrix in the form of a covariance matrix within an iterative procedure. In contrast to quasi-Newton methods the CMAES does neither approximate nor use gradients which makes the method feasible on multimodal and/or noisy problems. The CMAES achieve higher rates of convergence than other evolution strategies by employing evolution paths rather than single mutation steps in the adaptation process.

A detailed analysis of the advantages and limitations of the CMAES can be found in Hansen and Ostermeier (2001) and therefore we only present here an outline of the algorithm. In a  $(\mu, \lambda)$  CMAES, during every generation  $g$  a set of  $\lambda$  solutions  $\mathbf{x}_1^{g+1}, \mathbf{x}_2^{g+1}, \dots, \mathbf{x}_\lambda^{g+1}$  is constructed by sampling from an adapted random distribution and the best  $\mu$  individuals survive to the next generation  $g + 1$ . The  $\lambda$  solutions are constructed as

$$\mathbf{x}_k^{(g+1)} \sim \mathcal{N}\left(\langle \mathbf{x} \rangle_W^{(g)}, \left(\boldsymbol{\sigma}^{(g)}\right)^2 \mathbf{C}^{(g)}\right) \quad (7)$$

where

$\mathbf{x}_k^{g+1} \in \mathbb{R}^n$  is the object parameter vector of the  $k^{th}$  individual in generation  $g + 1$ .

$\langle \mathbf{x} \rangle_W^{(g)} := \frac{1}{\sum_{i=1}^{\mu} w_i} \sum_{i=1}^{\mu} w_i \mathbf{x}_{i:\lambda}^{(g)}$  is a weighted mean of the  $\mu$  best individuals of generation  $g$ . The index  $i : \lambda$  denotes the  $i^{th}$  best individual out of  $\lambda$  individuals.

$\boldsymbol{\sigma}^{(g)} > 0$  is the global step size in the generation  $g$ .

$\mathcal{N}(\mathbf{x}, \mathbf{C})$  is the multivariate normal distribution with mean  $\mathbf{x}$  and covariance matrix  $\mathbf{C}$

$\mathbf{C}^{(g)}$  is a symmetrical positive definite  $n \times n$  matrix that acts as covariance matrix for the multivariate normal distribution.  $\mathbf{C}$  is initialized to  $\mathbf{C}^{(0)} = \mathbf{I}$  and is adapted every generation using the evolution path.

The evolution path  $\mathbf{p}_c^{(g)}$  and the covariance matrix are adapted every generation as follows:

$$\mathbf{p}_c^{(g+1)} = (1 - c_c) \mathbf{p}_c^{(g)} + c_c \frac{c_W}{\boldsymbol{\sigma}^{(g)}} \left( \langle \mathbf{x} \rangle_W^{(g+1)} - \langle \mathbf{x} \rangle_W^{(g)} \right) \quad (8)$$

$$\mathbf{C}^{(g+1)} = (1 - c_{cov})\mathbf{C}^{(g)} + c_{cov}\mathbf{p}_c^{(g+1)} \left( \mathbf{p}_c^{(g+1)} \right)^T \quad (9)$$

where

$\mathbf{p}_c^{(g+1)} \in \mathbb{R}^n$  is the sum of weighted differences of points  $\langle \mathbf{x} \rangle_W^{(g)}$  i.e. the evolution path of the evolution strategy and is initialised to  $\mathbf{p}_c^{(0)} = 0$ .

$c_c \in ]0, 1]$  determines the cumulation step for the evolution path  $\mathbf{p}_c$ ,  $c_c^u := \sqrt{c_c(2 - c_c)}$  which normalizes the variance of  $\mathbf{p}_c$  and  $c_W = \frac{\sum_{i=1}^n w_i}{\sqrt{\sum_{i=1}^n w_i^2}}$

$c_{cov} \in [0, 1[$  is the rate of change of the covariance matrix  $\mathbf{C}$ .

The step size  $\sigma^{(g)}$  is also adapted using a conjugate evolution path as follows

$$\mathbf{p}_\sigma^{(g+1)} = (1 - c_\sigma)\mathbf{p}_\sigma^{(g)} + c_\sigma^u \mathbf{B}^{(g)} \left( \mathbf{D}^{(g)} \right)^{-1} \left( \mathbf{B}^{(g)} \right)^{-1} \cdot \frac{c_W}{\sigma^{(g)}} \left( \langle \mathbf{x} \rangle_W^{(g+1)} - \langle \mathbf{x} \rangle_W^{(g)} \right) \quad (10)$$

$$\sigma^{(g+1)} = \sigma^{(g)} \exp \left( \frac{1}{d_\sigma} \frac{\| \mathbf{p}_\sigma^{(g+1)} \| - \widehat{\chi}_n}{\widehat{\chi}_n} \right) \quad (11)$$

where

$\mathbf{p}_\sigma^{(g+1)} \in \mathbb{R}^n$  denotes the conjugate evolution path and is initialised to  $\mathbf{p}_\sigma^{(g+1)} = 0$

$c_\sigma \in ]0, 1[$  determines the cumulation time for  $\mathbf{p}_\sigma$  and  $c_\sigma^u = \sqrt{c_\sigma(2 - c_\sigma)}$

$d_{sigma}$  is a damping parameter for the step size which determines the possible change rate for  $\sigma$ .

$\widehat{\chi}_n = E[\| \mathcal{N}(\mathbf{0}, \mathbf{I}) \|] = \sqrt{2} \Gamma(\frac{n+1}{2}) / \Gamma(\frac{n}{2})$  is the expectation of a  $(\mathbf{0}, \mathbf{I})$  normally distributed random vector

$\mathbf{C}^{(g)} = \mathbf{B}^{(g)} \left( \mathbf{D}^{(g)} \right)^2 \left( \mathbf{B}^{(g)} \right)^T$  is a singular values decomposition of  $\mathbf{C}^{(g)}$ .

$\mathbf{D}^{(g)}$  is a  $n \times n$  diagonal matrix with  $d_{ij} = 0$  for  $i \neq j$  and the diagonal elements  $d_{ii}^g$  of  $\mathbf{D}^{(g)}$  are the square roots of the eigenvalues of the covariance matrix  $\mathbf{C}^{(g)}$ .

$\mathbf{B}^{(g)}$  is an orthogonal  $n \times n$  matrix whose columns are the normalized eigenvectors of  $\mathbf{C}^{(g)}$ .  $\mathbf{C}^{(g)}$  determines  $\mathbf{B}^{(g)}$  and  $\mathbf{D}^{(g)}$  apart from signs of the columns in  $\mathbf{B}^{(g)}$  and permutations of columns in both matrices.

Simulations on various test functions have revealed that the CMAES has local and global properties that outperform other search algorithms in particular for badly scaled non-separable functions where speed up factors of several orders of magnitude can be observed, see Hansen and Ostermeier (2001). Therefore this algorithm is tested next for the problem of inclusion detection in IRCAT.

## 5 Numerical results

In order to test the efficiency of the algorithm proposed, we consider the domain  $\Omega = \{(x, y) \mid (x^2 + y^2 < R^2)\}$ , with  $R = 2$ ,  $k = 1$  with an isotropic inclusion  $D$  parametrised given by a superellipse given by equation (5). The inclusions are also allowed to be rotated at an angle  $\theta_0$  with respect to the axes of coordinates and therefore there are seven parameters to be identified, namely  $x_0, y_0, a, b, p, q$  and  $\theta_0$ . The conductivity  $k$  is assumed to be known and for the purpose of this investigation it is fixed at  $k = 10$  but similar conclusions can be drawn using other values of  $k$ .

In order to calculate the value of the objective function (4) for a given possible solution for the inclusion  $D$ , an intermediate direct problem of the form (1)–(2) has to be solved. These intermediate direct problems are solved using a Boundary Element Method (BEM). For the problem of inclusion detection, the BEM is particularly suitable since the geometry of the system changes for every possible solution tested during the optimisation process. This reduces the computational effort and eliminates the important perturbations due to changes in the mesh. BEM also reduces the dimensionality of the problem by one by reducing the partial differential equation that governs the process to a boundary integral equation which involves only boundary data. Thus BEM provides clear advantages in comparison with other numerical methods to tackle this kind of inverse geometric problem. It should be noted that the boundary elements method is widely used for solving fault detection problems, see for example Aoki, Amaya, Urigo, and Nakayama (2005) or Forth and Staroselsky (2005). A BEM method with  $N_0 = 160$  boundary elements on the

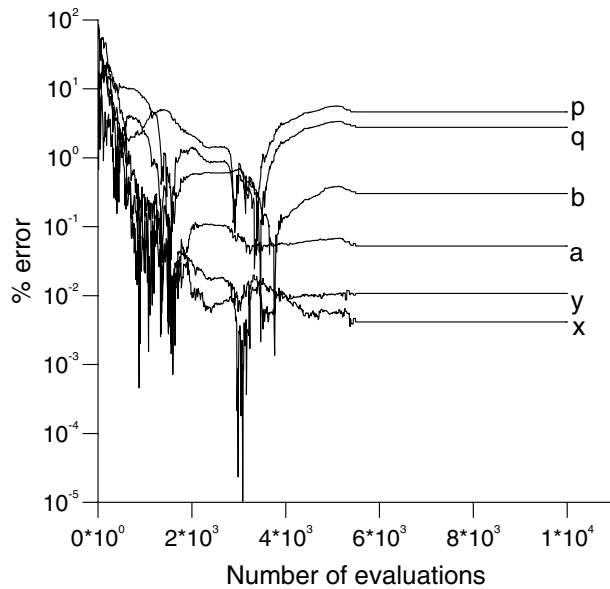


**Figure 2 :** The percentage errors obtained for predicting the parameters of a super-elliptical inclusion for the case of a circle given by  $x_0 = 1.0$ ,  $y_0 = 1.0$  and  $r_0 = 0.5$ .

outer boundary and  $N_1 = 80$  boundary elements on the inner boundary was used in order to ensure the accuracy of the numerical solution for the direct problem. Details about the numerical implementation of the BEM to solving direct problems of the form (4) can be found in Mera, Elliott, and Ingham (2003).

The (5,10)-CMAES algorithm presented in section 4 has been tested on several test examples. The results presented are averages obtained by running the CMAES 10 times for various sequences of random numbers in order to eliminate the variability generated by the stochastic nature of the algorithm. The control parameters of the evolutionary algorithms were set to default values.

First we consider the case of a circular inclusion given by  $x_0 = 1.0$ ,  $y_0 = 1.0$  and  $r_0 = 0.5$  and using the evolution strategy described in section 4 we search for a superellipse. The circle is accurately represented by a superellipse with  $a = b = r_0$  and  $p = q = 2$  and any rotation angle  $\theta_0$ . Thus we expect the CMAES to retrieve these values. Figure 2 shows the percentage errors in evaluating the super-elliptical parameters as functions of the number of objective function evaluations for a typical CMAES run. It can be seen that all the parameters are accurately predicted. It can also be seen that  $x_0$  and  $y_0$  are identified to

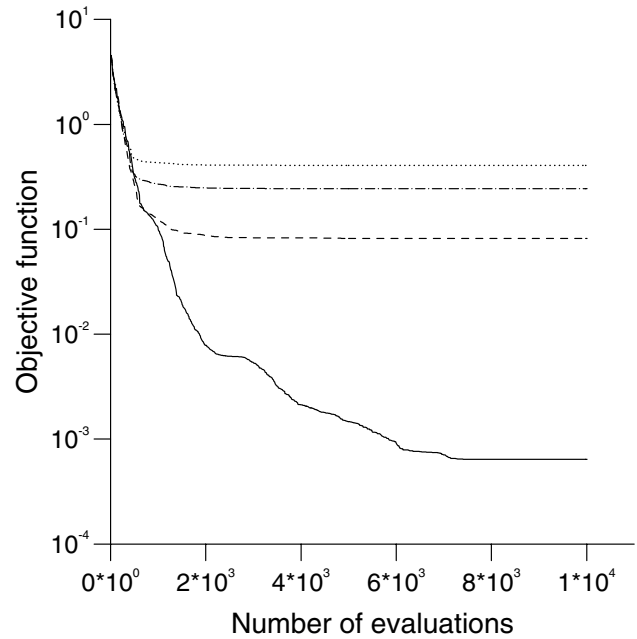


**Figure 3 :** The evolution of the objective function of best solution found by the CMAES as a function of the number of objective function evaluation for the test example given by a circle with  $x_0 = 1.0$ ,  $y_0 = 1.0$  and  $r_0 = 0.5$  for various levels of noise, namely  $s = 0\%$  (—),  $s = 1\%$  (- - -),  $s = 3\%$  (- · - · -) and  $s = 5\%$  (· · · · ·).

a greater accuracy than  $a$  and  $b$  and all these four parameters  $x_0, y_0, a$  and  $b$  are identified to a greater accuracy than  $p$  and  $q$ . Since  $x_0$  and  $y_0$  give the position of the inclusion,  $a$  and  $b$  indicate its size while  $p$  and  $q$  characterize the shape, it can be concluded that the position of the inclusion is easier to identify than the size of the inclusion and both the position and the size of the inclusion are easier to identify than its shape.

The evolution of the objective function obtained by the CMAES for the circular test example and various amounts of noise added into the input data in order to simulate the inherent measurement errors is presented in Figure 3 and the numerical solution obtained for the circular inclusion is presented in Figure 4. It can be seen that accurate results are obtained for various amounts of noise and that the algorithm proposed is convergent and stable with respect to increasing the amount of noise included in the input data. Figure 5 presents the CMAES generated solution in comparison with the exact solution for five different circular inclusions of various sizes and

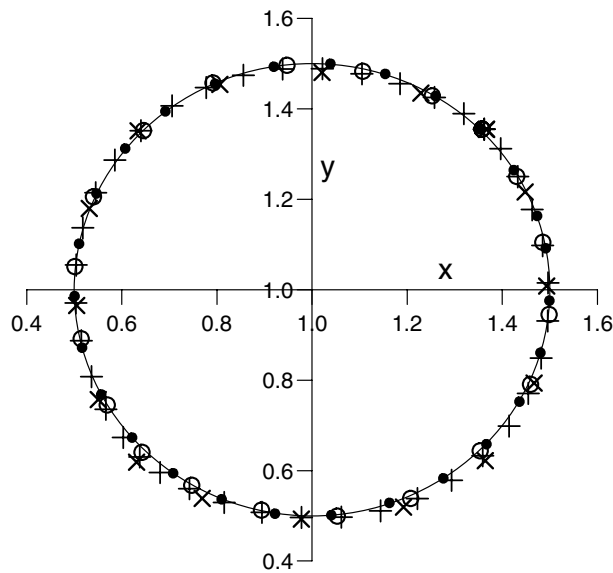


**Figure 4 :** The numerical solution found by the CMAES for a circular inclusion for various levels of noise, namely  $s = 0\%$  ( $\bullet$ ),  $s = 1\%$  ( $\circ$ ),  $s = 3\%$  ( $+$ ) and  $s = 5\%$  ( $\times$ ) in comparison with the exact solution given by  $x_0 = 1.0$ ,  $y_0 = 1.0$  and  $r_0 = 0.5$ .

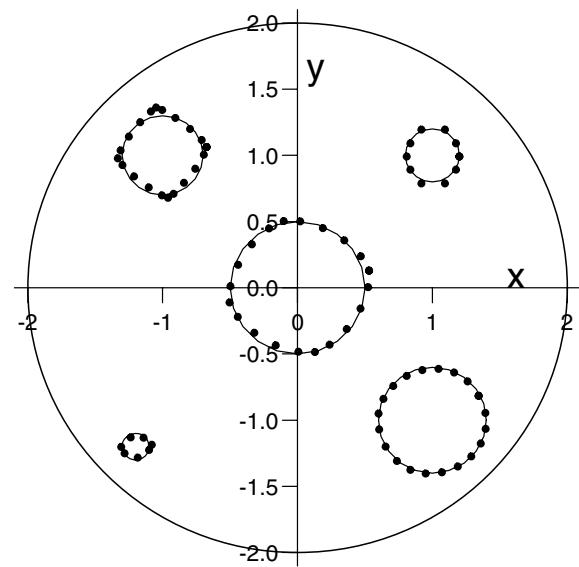


**Figure 5 :** The numerical solution obtained by the CMAES ( $\bullet$ ) for five test examples given by circular inclusions of various sizes and locations in comparison with the exact solution ( $—$ ). The five inclusions presented represent five single inclusion problems rather than one multi-inclusion problem.

locations. It should be noted that Figure 5 shows the results of five *different* problems, each consisting of the detection of a single circular inclusion, rather than the detection of five circles simultaneously. The results are presented on the same figure in order to limit the number of figures included in this paper. The numerical results have been obtained using 300 objective function evaluations and  $s = 5\%$  noise added into the input data. It can be seen that the circular inclusions are retrieved very accurately even if only a small number of objective function evaluations are used.

Figure 6 presents the CMAES generated solution in comparison with the exact solution for five different ellipses of different sizes, locations and orientations. Again, the five inclusions presented represent five single inclusion problems rather than one multi-inclusion problem. It can be seen that the elliptical inclusions are also retrieved very accurately.

Similar results are obtained for rectangular cavities see Figure 7 which presents the results for detecting a rectangular inclusion. The inclusion was again taken in five different positions and the results are presented on the same figure. Rectangular cavities are accurately identi-

fied, even if the super-elliptical representations only allows an approximate representation of rectangular cavities since an exact rectangle cannot be obtained for any values of  $p$  and  $q$ . From the results presented we may conclude that it is possible to accurately identify the position, the size, the shape and the orientation of inclusions of various shapes by using the super-elliptical parametrisation and the CMAES proposed in this paper.

## 6 Conclusions

In this paper an inverse geometric problem which requires the determination of the location and size of a super-elliptical inclusion  $D$  contained in a domain  $\Omega$  from temperature and heat flux measurements on the boundary  $\partial\Omega$  has been investigated numerically using super-elliptical parametrisation and a CMAES algorithm. Several test examples have been considered and it was found that the algorithm proposed is very efficient in locating an unknown inclusion even if no information about the shape of the inclusion is available. Overall, it may be concluded that the algorithm proposed is a robust, efficient and fast method for detecting the size and

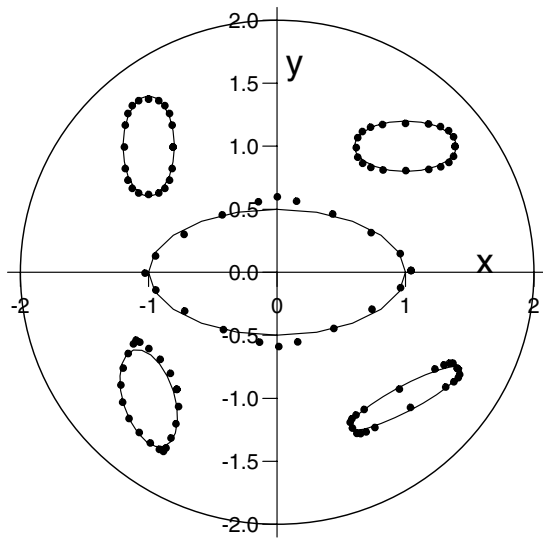


**Figure 6 :** The numerical solution obtained by the CMAES (●) for five test examples given by elliptical inclusions of various sizes and locations in comparison with the exact solution (—). The five inclusions presented represent five single inclusion problems rather than one multi-inclusion problem.

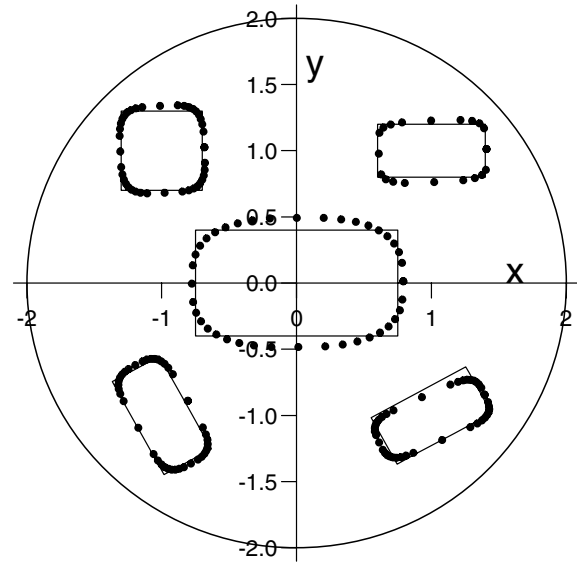


**Figure 7 :** The numerical solution obtained by the CMAES (●) for five test examples given by rectangular inclusions of various sizes and locations in comparison with the exact solution (—). The five inclusions presented represent five single inclusion problems rather than one multi-inclusion problem.

location of subsurface inclusions.

## References

- Aoki, S.; Amaya, K.; Urago, M.; Nakayama, A.** (2005): Fast Multipole Boundary Element Analysis of Corrosion Problems. *CMES: Computer Modeling in Engineering & Sciences*, vol. 6, no. 2, pp. 123–132.
- Forth, S.; Staroselsky, A.** (2005): A Hybrid FEM/BEM Approach for Designing an Aircraft Engine Structural Health Monitoring. *CMES: Computer Modeling in Engineering & Sciences*, vol. 9, no. 3, pp. 287–298.
- Gielis, J.** (2003): A Generic Geometric Transformation that Unifies a Wide Range of Natural and Abstract Shapes. *Amer. J. Botany*, vol. 90, pp. 333–338.
- Hansen, N.; Ostermeier, A.** (2001): Completely derandomized self-adaptation in evolution strategies. *Evolutionary computation*, vol. 2, pp. 159–195.
- Hsieh, C. K.; Su, K.** (1981): A methodology of predicting cavity geometry based on the scanned surface temperature data - prescribed heat flux at the cavity side. *J. of Heat Transfer*, vol. 103, pp. 42–47.
- Ikehata, M.; Ohe, T.** (2002): A numerical method for finding the convex hull of polygonal cavities using the enclosure method. *Inverse Problems*, vol. 18, pp. 111–124.
- Lesnic, D.** (2001): A numerical investigation of the inverse potential conductivity problem in a circular inclusion. *Inverse Problems in Engineering*, vol. 9, pp. 1–17.
- Mera, N. S.; Elliott, L.; Ingham, D. B.** (2002): Detection of subsurface cavities in IR-CAT by a real coded genetic algorithm. *Applied Soft Computing*, vol. 2, pp. 129–139.
- Mera, N. S.; Elliott, L.; Ingham, D. B.** (2003): A real coded genetic algorithm approach for subsurface isotropic and anisotropic inclusions detection. *Engineering Analysis with Boundary Elements*, vol. 11, pp. 157–173.

**Rus, G.; Gallego, R.** (2002): Optimization algorithms for identification inverse problems with the boundary element method. *Engineering Analysis with Boundary Elements*, vol. 26, pp. 315–327.